Insulin-like growth factor binding protein-related protein 1 (IGFBP-rP1) has a potential tumor- suppressive activity in human lung cancer

Yuan Chen[1], Fei Ye [1], Manuela Pacyna-Gengelbach[1], Thomas Knösel[l], Nicole Deutschmann[1], Per Lund[1], Hiroaki Yasumoto[2] , Tsuguru Usui[2] and Iver Petersen[1]*

[1]Institute of Pathology, University Hospital Charité, Schumannstr 20-21, D-10098 Berlin, Germany

[2] Department of Urology, Graduate School of Biomedical Sciences, Hiroshima University, Hiroshima, Japan;

The work was supported by a grant from the Deutsche Krebshilfe (grant 10-2210-Pe 4).

Running title: Tumor suppressor IGFBP-rP1 in lung cancer

Key words: IGFBP-rP1, human lung cancer, DNA methylation, stable transfection, tumor suppressor, differentiation

The abbreviation used are: IGF, insulin-like growth factor; IGFBP-rP1: insulin-like growth factor binding protein-related protein 1; HBEC: Human bronchial epithelial cell; SAEC: small airway epithelial cell; BrdU: 5-bromodeoxyuridine; TMA: Tissue microarray; 5-aza-dCyd: 5-aza-2'-deoxycytidine

*Correspondence to:
Dr. Iver Petersen, MD
Institute of Pathology
Charité Medical School
Humboldt-University
D-10098 Berlin, Germany Tel: +49-30-450536050
Fax: +49-30-450536902
Email: iver.petersen@charite.de

Abstract

Insulin-like growth binding protein-related protein 1 (IGFBP-rP1) has decreased expression in various tumors, but the role of IGFBP-rP1 in lung cancer has not yet been elucidated. In this study, we evaluated the IGFBP-rP1 expression in lung cancer cell lines and we found a reduced expression of IGFBP-rP1 at both mRNA and protein levels. In a tissue microarray containing 138 primary tumors analyzed by immunohistochemistry, 58 cases (42%) exhibited no expression of IGFBP-rP1, additionally, an association between IGFBP-rP1 expression and tumor gradings was found in squamous cell lung cancer. Neither deletion or gene rearrangement nor loss of heterozigosity was responsible for the inactivation of IGFBP-rP1. However, 5-aza-2'-deoxycytidine treatment restored the expression of IGFBP-rP1 in 3 out of 4 lung cancer cell lines. Sequencing of sodium bisulfite–treated genomic DNA from these 3 lung cancer cell lines revealed a heterogeneous methylation pattern in the region of exon 1 and intron 1. Stable transfection of IGFBP-rP1 full-length cDNA into a lung cancer cell line H2170 led to an increased protein expression of IGFBP-rP1. IGFBP-rP1 positive transfectants remarkably reduced the ability of colony formation in soft agar, suppressed the tumor growth rate in nude mice and increased the number of apoptotic cells as well as the expression level of casepase-3 compared to controls. Moreover, treatment with differentiation modulating agent 5-bromodeoxyuridine (BrdU) led to an enhanced expression of IGFBP-rP1 in lung cancer cells. Out data suggest that IGFBP-rP1 is a tumor suppressor possibly via DNA methylation and induction of apoptosis in human lung cancer.

Introduction

The insulin-like growth factor (IGF) signalling pathway plays a key role in regulating proliferation, differentiation, and apoptosis in mammalian organisms (1). The IGF system is made up of a series of members including IGF-I, IGF-II, IGF receptor-I, IGF receptor-II, IGFBPs (IGFBP-1 to 6), IGFBP-rPs (IGFBP-rP1 to 10), and IGFBP proteases. IGFBP-rP1, also named mac25, tumor-derived adhesion factor, prostacyclin-stimulating factor or IGFBP-7, was initially identified to be differentially expressed in normal leptomeningeal and mammary epithelial cells compared to their counterparts (2,3). IGFBP-rP1 shares about 30% identity at the amino acid level with the IGFBPs, but exhibits low affinity with IGFs, with a 5- to 6-fold lower affinity for IGF-I and a 20- to 25-fold lower affinity for IGF-II, in comparision to IGFBP-1 to 6 (4-6).

Although the biological roles of IGFBP-rP1 have not been well established, a study about the characterization of the normal distribution of IGFBP-rP1 showed that the protein has a highly restricted pattern of expression within a given tissue, allowing the analysis of changes in corresponding neoplasms (7). Indeed, a growing body of evidence suggests that IGFBP-rP1 may act as a tumor suppressor in various cancer types. For example, the expression of IGFBP-rP1 was found to be reduced in uterine leiomyomata compared with adjacent myometrium (8). Decreased IGFBP-rP1 expression was observed in prostate cancer and the restoration of IGFBP-rP1 expression by transfecting it into prostate cancer cell lines was shown to dramatically reduce tumorigenic potential of the cell lines (9,10). In breast cancer, IGFBP-rP1 was implicated as a senescence-associated factor, and moreover, the downregulation of IGFBP-rP1 was found to be associated with inactivation of the retinoblastoma protein, cyclin E overexpression and increased proliferation of breast cancer cells (3,11-12). In liver cancer, diminished expression of IGFBP-rP1 was explained by promoter hypermethylation (13).

Previously, we performed suppression subtractive hybridization (SSH) to identify lung cancer-associated genes when comparing gene expression between human bronchial epithelial

cells (HBEC) and lung cancer cell lines (14,15). Several cDNA libraries enriched for genes that were downregulated or upregulated in lung cancer cell lines were established. The clone HBEC383 isolated from the library containing the genes underexpressed in lung cancer, shared high similarity to human IGBFP-rP1. As the expression of IGFBP-1 to 6 has been shown to be modified in lung cancer (16,17), while little is known about the possible tumor-inhibitory roles of IGFBP-rP1 in lung cancer, we are particularly interested in looking at the expression pattern as well as the biological role of IGFBP-rP1 in lung cancer. In this study, we analyzed the expression of IGFBP-rP1 in lung cancer cell lines and in primary lung tumors, explored the mechanism responsible for the downregulaton of IGFBP-rP1, and investigated the possible biological function of IGFBP-rP1 in human lung cancer.

Materials and Methods

Cell lines and primary cell culture

Human bronchial epithelial cells (HBEC) and human small airway epithelial cells (SAEC) were purchased from Clonetics (San Diego, CA) and cultured in BEG or SAB media (Clonetics) until population doubling of maximal 10. Human lung carcinoma cell lines including small cell lung carcinomas (SCLCs: COLO668, COLC677, H526, DMS79, H82, SHP77, CPC-N) and non small cell lung carcinoma (non-SCLCs: H2170, H125, H123, H2030, H226, BEN, H2228, H23) were bought from the American Type Culture Collection (ATCC, Rockville, MD) or from the German Collection of Microorganisms and Cell Culture (DSMZ, Braunschweig, Germany). Additionally, 4 NSCLC cell lines, D51, D54, D97 and D117 were established in our lab. They were derived from primary tumors of patients who were operated at the Charité University Hospital. These cells were grown in Leibovitz 15 media supplemented with 10% FCS and 1% glutamine.

Treatment of demethylation agent 5-aza-2'-deoxycytidine (5-aza-dCyd)

To investigate the effect of demethylation agent 5-aza-2'- deoxycytidine (Sigma Chemical Co., St. Louis, MO), four lung cancer cell lines including H2170, H226, SHP77 and H2030 lacking the expression of IGFBP-rP1 were selected for demethylation test. Cells were seeded at a density of 9×10^5 in 100-mm dishes until 50% confluency was achieved and were treated with 0, 10, 20 25 μM 5-aza-dCyd for 48 hours. Then the cells were washed with phosphated-buffered saline (PBS) and incubated further in fresh medium containing the same concentration of 5-aza-dCyd for 48 hours before isolation of total RNA. The gene expression level was measured by RT-PCR as described below.

Evaluation of DNA methylation by sequencing of sodium bisulfite–treated DNA

Treatment of genomic DNA from lung cancer cell lines with sodium bisulfite was performed as described previously (18). Bisulfite-treated DNA was subjected to PCR, resulting in a PCR product of 186-bp (+464 to +649) spanning 19 CpG sites of exon 1 and intron 1 region. The target fragment was amplified using the primer pair: 5'-GGGGAGAAGGTTATTATTTAGGTTAGTAA-3' (sense) and 5'-CCCTCCCATCTAACTCCTAAAATAC-3' (antisense). The PCR conditions were as follows: 95°C for 15 minutes, 36 cycles of 95°C for 1 min, 54°C for 1 min and 72°C for 1 min, with final extension at 72°C for 10 minutes. PCR products were subcloned into the T/A cloning vector pCR2.1 (Invitrogen, Karlsruhe, Germany) and then sequenced with M13 reverse primer as previously described.

Modification of lung cancer cell lines with differentiation inducing agent, 5-bromodeoxyuridine (BrdU).

To study the role of IGFBP-rP1 in lung cancer differentiation, three lung cancer cell lines, H2228 (NSCLC), COLO668 (SCLC) and H526 (SCLC), were treated with differentiation inducing agent BrdU.

Adherent cells of H2228 and COLO668 were seeded at a density of 9×10^5 in 10 mm dishes. Twenty-four hours later, H2228 cells were treated with 0, 10 and 20 µM BrdU, while for COLO668 the working concentrations of BrdU were 0, 0.1 and 0.5 µM according to the cell growth curve (data not shown).

The floating SCLC cell line H526 was treated with 2.5 µM BrdU for 8 weeks. BrdU treatment led to the appearance of substrate-adherent cells. The floating cells were aspirated and the adherent cells, called H526B, were grown in the absence of BrdU. Afterwards, cells were harvested and RNA was isolated for RT-PCR and Western blot analysis.

DNA fingerprinting

Genomic DNA was isolated from the cultured cell lines H526 and H526B according to standard protocol (proteinase K digestion, phenol/chloroform extraction, and ethanol precipitation). DNA fingerprinting was carried out with the random amplified polymorphic DNA (RAPD) method (19). PCR products were resolved by electrophoresis on a 1.5% (w/v) agarose gel and visualized by ethidium bromide staining.

Northern blot analysis

Ten µg of total RNA extracted from HBEC, SAEC, and lung tumor cell lines (H2170, D54, H125, H123, SHP77, H2030, D117, D51, D97, CoLo677, CoLo668, H82, BEN, H226, DMA79 and H526) were separated in 1.2% agarose/2.2 M formaldehyde gel and run for 4 hr at 60V followed by capillary transfer onto nylon membranes (Amersham, Braunschweig, Germany) overnight. A Northern blot of poly $(A)^+$ RNA from different human tissues (Human 12-lane MTN blot, #7780-1) was obtained from Clontech (Germany). The cDNA clone of HBEC383 was amplified by nested PCR as described previously (15) and used as probe labeled by random priming with [^{32}P]-dCTP (Megaprime labelling, Amersham). Following at least 30 min of prehybridization with Expresshyb solution (Clontech), the denatured probe was added and hybridization was carried out at 58°C overnight. Blots were washed with 2x SSC/0.1% SDS at room temperature and 0.1x SSCP/ 0.1% SDS at 60°C and exposed to X-ray films at –80°C.

Semi-quantitative RT-PCR

Total RNA was prepared from the HBEC, SAEC, and lung tumor cell lines by using Trizol (Life Technologies, Gaithersburg, MD) and then incubated with RQDNaseI (Progema, Madison, WI) for 40 min at 37°C.

First-strand cDNA was reverse-transcribed by 200 U superscript II transcriptase (Gibco, Eggenstein, Germany) from 2 µg of total RNA, in the presence of 1× RT buffer, 100 mM DTT, 20 U RNase inhibitor and 5 mM dNTPs, using the random hexamer primers supplied in the kit according to manufacturer's protocol. Reactions lacking reverse transcriptase were used to verify the absence of amplification from genomic DNA contamination (data not shown). The following primers were used for PCR amplification: IGFBP-rP1 primers (forward: 5′-CATCACCCAGGTCAGCAA-3′ and reverse: 5′-TGGAGGTTTATAGCTCGG-3′); caspase 3 primers (forward: 5'-CAAACTTTTTCAGAGGGGATCG-3'; caspase-3 reverse, 5'-GCATACTGTTTCAGCATGGCA-3'. PCR conditions were 94°C 1 min, 52°C 30 sec and 72°C 30 sec, for 33 cycles, with initial denaturation at 95°C 5 min and final elongation at 72°C 5 min. Controls were performed with commercially available glyceraldehyde-3-phosphate dehydrogenase (GAPDH) primers (Clontech).

Tumor tissues

Tumor specimens from 138 patients with lung cancer were used for construction of tissue microarrays. In addition, 29 paired normal/tumor tissues were applied for the analysis of loss of heterozygosity (LOH). All of these patients were undergoing surgical operation of lung cancer at the Department of Surgery of Charité University Hospital from 1995 to 2000. No adjuvant radiotherapy or chemotherapy was administered before surgery. For LOH analysis, the specimens were frozen in liquid nitrogen and stored at -80°C before genomic DNA isolation. The clinicopathological characteristics of the samples were listed in Table 1 according to TNM criteria of the UICC (20).

Tissue microarray construction and immunohistochemical analysis

Tissue microarrays (TMAs) were constructed with assistance of Oligene (oligene GmbH, Berlin, FRG) using a manual tissue arrayer purchased from Beecher Instruments (Woodland, USA). All sections were reviewed by two pathologists (T Knösel and YW Yu). Suitable areas for tissue retrieval were marked on standard haematoxylin and eosin (H&E) sections. Tissue cylinders with a diameter of 0.6 mm were punched out of the paraffin block and transferred into a recipient array block. After construction, 4 µm sections containing 276 tumors from 138 patients were cut from the 'donor' blocks and transferred to glass slides without any sectioning aids.

Immunohistochemistry was carried out as described previously (18). Polyclonal rabbit anti-IGFBP-rP1 antibody (Immunological & Biochemical testsystems GmbH, Germany) was used at 1:200 dilution. Three large sections from normal lung tissue were used as controls. All slides were manually read by one pathologist (T Knösel) who was blinded to the clinical information. Immunohistochemistry was scored semiquantitatively as negative (score 0), weak (score 1), moderate (score 2) or strong (score 3) as previously described. For statistical evaluation, scores 0-1 were therefore considered as negative and scores 2-3 as positive.

LOH analysis

Twenty-nine paired samples of tumor and normal DNA were assessed for allelic loss by microsatellite polymorphism analysis. Three microsatellite markers including D4S189 (4p15-q23), D4S231 (4q11-q31) and D4S392 (4q12-q12) were chosen for LOH analysis. Primer sequences were obtained from the genome database and commercially synthesized (MWG-Biotech, Ebersberg, Germany). For LOH-analysis, one primer was labelled with the IRD700 infrared dye. PCR was performed as previously described and the DNA fragments were finally visualized by non-radioactive detection (19). LOH was determined when the allele of the tumor sample was less than 50% in comparison to the normal DNA.

Construction of expression vector and transfection

IRES 2 neo expression vector containing the full-length coding sequence of IGFBP-rP1 was constructed as previously described (9). The IRES 2 neo/IGFBP-rP1 expression vector was digested with EcoR I and Kpn I, afterwards, the 1.1- kb fragment of the IGFBP-rP1 insert was subcloned into an EcoR I/Kpn I restriction site of the mammalian expression vector pcDNA3.1 (Invitrogen).

To obtain stable transfectants, lung cancer cells H2170 were seeded at a density of 9 x 10^5 cells in 100-mm dishes, cultured for 24 hours, and transfected with 8 µg of pcDNA3.1/IGFBP-rP1 and 40 µg of lipofectin (Invitrogen) according to the manufacturer's recommendation with a slight modification. Empty vector was transfected as a control. β-galactosidase was assayed to control transfection efficiency. Forty-eight hours after transfection, G418-resistant clones were selected by the addition of G418 at 0.4 mg/ml to the culture medium for 2 to 3 weeks.

Western blot analysis

Western blot analysis was performed to detect IGFBP-rP1 in cultured media or in cell lysates. Briefly, media from cells were collected and normalized based on cell counts and then concentrated by filtration through nitrocellulose (Milipore, Germany). After concentration, proteins were redissolved in 50 µl of SDS sample buffer containing 0.5 M Tris (pH 6.8), 1% SDS, 10% glycerol, 0.003% bromphenol blue and 8 M urea by heating for 10 min at 95°C. Proteins from cell lysates were isolated according to standard protocol. Samples were electrophoresed on 12% SDS-polyarcylamide gels and electroblotted onto nitrocellulose. Polyclonal anti-IGFBP-rP1 antibody was used at a 1:1000 dilution. Signal was visualized with alkaline horseradish peroxidase–conjugated goat anti-rabbit antibody (1:1000; DAKO, Hamburg, Germany) and enhanced chemiluminescence detection system (Amersham,

Freiburg, Germany) according to standard procedures. As loading control, rabbit anti-actin antibody was used at a concentration of 1:1000 (Chemicon).

Soft Agar Assay

To analyze anchorage-independent growth of IGFBP-rP1 transfectants and control empty vector-transfected H2170 cells, 40-mm dish was first layered with 1% agar/2X RPMI with 10% FCS. A top layer containing 15×10^3 cells/dish suspended in 2x RPMI supplemented with 10% FCS and 0.5% agar was added. Assays were performed in duplicate. Colonies were counted 4 weeks after seeding in soft agar.

Tumorigenecity assay

For testing tumorigenicity in nude mice, suspensions of 1×10^6 cells from the two IGFBP-rP1 transfectants N6 and N10, the empty vector transfectant M12 as well as the parental cell line H2170 in a volume of 0.2 mL of serum-free culture medium were injected s.c. into 5- to 8-week-old female immune-deficient nude mice (Shoe:NMRI-*nu/nu*) purchased from Charles River Laboratories (Massachusetts, USA). Mice were divided into 4 groups according to the 4 cell lines tested. Each group contained three mice which received the injection of the same cell line. Mice were then monitored weekly for tumor formation for 8 weeks. If tumors were present, tumor volume was calculated using the formula: $(l \times w^2)/2$ (where l = length and w = width of tumor). Cell populations were considered to be nontumorigenic if no tumors were detected after 5 months postinjection.

Apoptosis assay

Starved cells of H2170, IGFBP-rP1 transfectants N6 and N10 and control empty vector-transfected cells M12 were seeded in 96-well plates (3000 cells/well) and cultured in 200 µl RPMI serum-free medium. After 72 h, cultured medium was replaced with fresh RPMI

medium containing APOPercentage Dye Label (Biocolor Ltd., United Kingdom) and incubated for 30 min at 37°C. Purple-red stained cells were identified as apoptotic cells and the number of apoptotic cells/100 cells was counted.

Statistical analysis

To compare the protein expression of IGFBP-rP1 with clinicopathologic parameters, 2 x 2 contingency tables (e.g. IGFBP-rP1 negative and IGFBP-rP1 positive and G1&G2 versus G3) were set up and the χ^2 test was applied. For apoptosis assay, the number of apoptotic cells between IGFBP-rP1 transfectant and controls was calculated by using the Student's *t* test. All analyses were done using the statistical software package SPSS 11.5 and *P* values <0.05 were considered statistically significant.

Results

Expression analysis of IGFBP-rP1 in cultured lung cancer cell lines

IGFBP-rP1 mRNA expression was analyzed in 19 lung cancer cell lines by using Northern blot analysis together with RT-PCR (Fig. 1A, 1B). We found that IGFBP-rP1 was downregulated in most of the lung cancer cell lines tested compared to normal controls of HBEC and SAEC. Especially for the cell lines H2170, H125, SHP77, H2030, D117, H82, BEN, H226, DMS79 and H526, there was no clear signal detectable. In good agreement with mRNA expression of IGFBP-rP1, Western blot analysis showed that IGFBP-rP1 protein expression markedly decreased or lost in lung cancer cell lines of COLO677, H526, H2170, COLO668 and H2228 (Fig. 1C).

Expression analysis of IGFBP-rP1 in lung primary tumors

A tissue microarray was constructed to explore the IGFBP-rP1 protein expression in 276 primary lung cancer samples representing 138 patients. Figure 2A shows one section of the TMA. In the tumor samples, 58 cases (42%) exhibited no relevant IGFBP-rP1 staining (Fig. 2B), while in the other 80 cases (58%), the IGFBP-rP1 staining was positive with the signals localizing in cytoplasm (Fig. 2C-E). The expression of IGFBP-rP1 did not differ significantly by tumor stage, tumor size and nodal status. However, there was a correlation between decreased IGFBP-rP1 expression and tumor gradings (G1 and G2 versus G3) in squamous cell lung cancer. The tumors with higher grading exhibit lower expression of IGFBP-rP1 protein, reaching statistical significance ($p = 0.029$).

On analyzing of 65 lung cancer patients with a median 24 months survival (range 2-66 months), we found no significant effect of IGFBP-rP1 protein expression on overall survival ($p= 0.30$; Kaplan-Meier statistical analysis).

LOH analysis

LOH analysis was carried out in 29 paired normal lung and tumor tissues. We found that for the microsatellite marker D4S189, LOH occurred in 4 out of 23 informative cases, similarly, for the marker D4S231 and D4S392, only 2 and 3 cases respectively, exhibited LOH (data not shown).

Reexpression of IGFBP-rP1 in lung cancer cell lines after 5-aza-dCyd treatment

To investigate whether the lack of expression of IGFBP-rP1 in tumor cells is associated with DNA hypermethylation, we treated four cell lines including H2170, H226, SHP77 and H2030 with increasing concentrations of the DNA methyltransferase inhibitor 5-aza-dCyd and measured IGFBP-rP1 mRNA expression by RT-PCR. As shown in Fig. 3, the expression of IGFBP-rP1 was restored in three cell lines of H2170, H226 and SHP77. In H2170, reexpression increased with rising concentration of 5-aza-dCyd. Compared to H2170, the reexpression of IGFBP-rP1 in H226 and SHP77 was, however, not in a dose-dependent manner.

Analysis of the methylation status in lung cancer cell lines

The methylation status of the IGFBP-rP1 gene in lung cancer was determined by PCR after bisulfite treatment of DNA followed by sequencing of the PCR products. We amplified a 186-bp fragment in the region of exon 1 and intron 1 spanning 19 CpG sites and analyzed the methylation status in 20 colonies from the lung cancer cell line H2170, H226 and SHP77 respectively. The target fragment of 186-bp was only observed in bisulfite treated genomic DNA but not in the unmodified DNA, indicating a successful modification of the DNA by the bisulfite treatment (Fig. 3B). Sequencing analysis showed that methylation occurred in all three cell lines and all the colonies analyzed, among which a heterogeneous methylation pattern was found (Table 2). The hotspots sites were concentrated on +541, +544, +548, +556,

+569, +581 and +586. Compared to cell line H2170 and H226, methylation occurred most frequently in cell line SHP77. Additionally, for normal cells of HBEC, we randomly picked out 10 colonies for sequencing, but did not find any methylation within the CpG dinucleotides.

Characterization of Stable Transfectants

To further examine the possible biological role of IGFBP-rP1 in lung cancer, we transfected the tumor cell line H2170 with the mammalian expression vector pcDNA3.1/IGFBP-rP1 containing the whole coding region of the gene. Colonies showing resistance against G418 were selected and further characterized. IGFBP-rP1 expression in different clones was measured by Western blotting (Fig. 4A). We selected two IGFBP-rP1 transfectants named N6 and N10 which showed higher expression of IGFBP-rP1 compared to mock transfectant (empty vector) and the parental cell line H2170 for the soft agar test, tumorigenecity assay and apoptosis assay.

Effect of IGFBP-rP1 on anchorage-independent growth of transfected and control Cells.

In soft agar test, we observed a reduced capacity of IGFBP-rP1 transfectants N6 and N10 to form colonies compared to mock transfectant and parental cells. After 4 weeks of incubation in soft agar, fewer colonies as well as smaller size of colonies formed by the transfectants N6 and N10 compared with the control clones and parental cells (Fig.4B).

Tumor formation in vivo

Mice were monitored weekly for tumor formation over an 8-week period. Mice that were given injection of the IGFBP-rP1 transfectants had lower tumor growth rate compared to those receiving the injection of mock transfectant or parental tumor cells (Fig. 4C). Especially for the IGFBP-rP1 positive transfectant N10, no tumor developed in each of 3 mice after 8 weeks. The mice were further observed for 3 months, however, still no tumor grew.

Effect of IGFBP-rP1 expression on apoptosis of H2170 cells.

To elucidate a potential influence of IGFBP-rP1 on apoptosis in human lung cancer cells, we performed APOPercentage assay to determine the relationship between IGFBP-rP1 expression and apoptosis in the IGFBP-rP1 cDNA-transfected H2170 cells, control empty vector and parental cells. As shown in Fig. 5A and 5B, the number of apoptotic cells which stained purple-red in the IGFBP-rP1 transfectant N10 (42 of 100 cells) was significantly higher than that in mock transfected cells (8 of 100 cells) or parental cells (4 of 100 cells). For the other IGFBP-rP1 transfectant N6, the number of apoptotic cells was slightly higher (10 of 100 cells) than in control, which however did not reach statistical significance.

To further confirm the role of IGFBP-rP1 in apoptotic lung cancer cells, we analyzed the mRNA expression of caspase-3 in IGFBP-rP1 transfectants N6, N10 and control cells. We found that caspase-3 was strongly expressed in transfectant N10 and slightly expressed in N6 compared with controls (Fig. 5c).

Effect of IGFBP-rP1 on lung cancer differentiation

BrdU has been used to induce differentiation in a variety of tumor cell lines including melanoma, neuroblastoma and lung cancer cell lines (22-24). To elucidate the role of IGFBP-rP1 in lung cancer differentiation, we established a differentiation cell-model by exposure of lung cancer cell lines including H2228, H526 and COLO668 to differentiation modulating agent BrdU. After that, the expression of IGFBP-rP1 was evaluated in the cell-model.

Interestingly, a striking morphological difference between H526 and H526B turned out after BrdU modification. When cultured in vitro, SCLC cell line H526 grows as floating cell aggregates (Fig. 6A). After BrdU treatment, adherent cells termed H526 B appeared among the floating cells (Fig. 6B).

DNA fingerprinting was carried out and we found that for all primer sets, distinctive banding patterns were detectable, however, for the same primer set, the DNA banding pattern between

H526 and H526B was identical (Fig. 6C). This result indicated that the subpopulation of H526B did not result from contamination by other adherent cells but was indeed induced by cell differentiation. H526 and H526 B were genetically identical.

The utility of this cell-model was confirmed by analyzing the expression of several lung differentiation markers such as surfactant protein C, Connexin26 and PITX1 (data not shown). Afterward, RT-PCR and Western blotting were performed to analyze the expression of IGFBP-rP1 in the cell-model. It turned out that IGFBP-rP1 was upregulated at both mRNA and protein levels in cell line H2228 and H526 after BrdU treatment, suggesting the involvement of IGFBP-rP1 in lung cancer differentiation (Fig. 6D, Fig. 6E).

Discussion

IGFBP-rP1 is distributed in a wide range of different human tissues, but its expression was reduced or lost in various tumor cell lines (9-13). In lung cancer, the functional role and regulatory mechanism(s) of IGFBP-rP1 have not yet been investigated. In this study, we analyzed the IGFBP-rP1 gene which was identified in our SSH screening for differentially expressed genes between human bronchial epithelial cells (HBEC) and a lung squamous cancer cell line H2170. It was of interest that IGFBP-rP1 was downregulated not only in the cell line H2170 used for the SSH library construction, but also was underexpressed in a panel of lung cancer cell lines tested. Considering its chromosomal location of 4q12, a region found to be frequently deleted in lung cancer, and its potential tumor suppressive functions in prostate cancer, breast cancer and liver cancer, we focused on the role of IGFBP-rP1 in lung cancer.

We first analyzed the expression of IGFBP-rP1 in lung cancer cell lines as well as in primary lung tumors, and we found that IGFBP-rP1 expression was decreased in a majority of lung cancer cell lines at both mRNA and protein levels compared to normal control. In primary lung tumors, 58 out of 138 cases (42%) exhibited no expression of IGFBP-rP1 protein. This observation is in good agreement with those reported in breast, prostate and liver cancer, where IGFBP-rP1 was strongly expressed in normal tissues but downregulated in their counterparts. Moreover, a significant association between the IGFBP-rP1 protein expression and tumor gradings was found in squamous cell lung cancer (SCC). SCC patients with higher grading showed relatively low expression of IGFBP-rP1 protein suggesting the involvement of IGFBP-rP1 in lung cancer differentiation and progression.

The mechanism of loss of IGFBP-rP1 expression in cancer cells is not fully understood, however, deletion, mutation or gene rearrangement is obviously not the common event for the inactivation of IGFBP-rP1, since so far no deletion, mutation or gene rearrangement of IGFBP-rP1 has been reported in any type of cancers. On the contrary, the loss of

heterozygosity of the IGFBP-rP1 gene is a frequent genetic event in breast cancer (25) and DNA hypermethylation of IGFBP-rP1 seems to be linked to its downregulation in prostate cancer and in hepatic carcinoma (9,13). In lung cancer, promoter hypermethylation of the IGFBP-3 gene, another member of the IGF superfamily, was thought to be responsible for the loss of the IGFBP-3 gene expression (26). To determine if genetic mechanisms participate in gene silencing, we performed LOH analysis as well as Southern blot analysis. No deletion or gene rearrangement was found and only very few cases showed LOH. The expression of IGFBP-rP1 was restored in 3 out of 4 lung cancer cell lines after they were exposed to demethylation agent, 5-aza-2'-deoxycytidine. The methylation status of IGFBP-rP1 was further evaluated by sequencing of sodium bisulfite–treated genomic DNA from the 3 lung cancer cell lines. A heterogeneous methylation pattern in IGFBP-rP1 turned out, lending support that 5-aza-dCyd–dependent increase of the IGFBP-rP1 gene expression occurs directly, not through effects at other loci, in a way that the IGFBP-rP1 gene expression is regulated by another protein that itself is methylated. Thus, the downregulation of IGFBP-rP1 in lung cancer could be explained by DNA hypermethyation of CpG inlands. To our knowledge, this is the first report providing direct evidence of DNA hypermethylation of IGFBP-rP1 in cancer cells by sequencing of the bisulfite–treated genomic DNA.

Early studies showed that overexpression of IGFBP-rP1 in prostate cancer cell lines resulted in increased doubting time, decreased colony formation and reduced tumor growth in nude mice (9,10). To investigate the function of IGFBP-rP1 in lung cancer, we stably transfected the lung cancer cell line H2170 with full-length cDNA of this gene. We selected H2170 for transfection based on three reasons. First, H2170 was applied for the construction of the SSH libraries. Second, there is no endogenous IGFBP-rP1 expression in H2170 which was confirmed by Northern blot and Western blot analysis. Third, treatment of H2170 with 5-aza-2'-deoxycytidine restored the expression of IGFBP-rP1. After transfection, we found that the obtained transfectants N6 and N10 displayed high IGFBP-rP1 protein expression levels

correlated with impaired ability of anchorage-independent growth *in vitro* and suppression of tumorigenicity in nude mice, and moreover, increased the number of apoptotic cells through upregulation of the caspase-3 gene compared with the mock transfectant and cancer cells. Thus, expression analysis and *in vitro* as well as *in vivo* growth characteristics are compatible with a role of IGFBP-rP1 as a tumor suppressor in lung cancer.

IGFBP-rP1 is a member of IGF superfamily with the exhibition of a low affinity to IGF-I and IGF-II. Although the influence of IGFBP-rP1 on the action of IGFs has been reported (27,28), the evidence suggesting a predominant IGF-independent role for IGFBP-rP1 is intensive. For example, Mutaguchi et al. found that the growth rate of transfected prostate cancer cells PC-3-rP1 and control PC-3 cells did not change by treatment with IGF-I in the culture medium (9). Oh et al. treated Hs578 T cancer cells with baculovirus-expressed IGFBP-rP1 and observed that the treatment resulted in inhibition of DNA synthesis and cell proliferation in a dose-dependent manner, even in the absence of IGF peptides (29). In the present study, we treated IGFBP-rP1 positive transfectants N6 or N10 as well as control cells with IGF-I, however, no change on the growth rate of the cells turned out (data not shown). Therefore, it seems likely that IGFBP-rP1 exerts its tumor suppressive function through IGF-independent pathway in lung cancer.

Studies of IGFBP-rP1 and its ability to induce apoptosis independent of IGF in PC-3 and M12 prostate cancer cells hint to a possible mechanism for IGFBP-rP1 as a tumor suppressor in other cancer cells (9,10). Additionally, the overexpression of the other two IGF superfamily members, IGFBP-3 and IGFBP-6, has been reported to inhibit the growth of non-small-cell lung cancer (NSCLC) cells by inducing apoptosis (30-32). Indeed, after transfection of IGFBP-rP1 into the lung cancer cell line H2170, we found that the number of apoptotic cells was significantly increased in IGFBP-rP1 positive transfectant N10 and correspondingly, N10 cells showed more expression of caspase-3 mRNA compared to controls, raising the

possibility that IGFBP-rP1 has a tumor-suppressive activity through induction of apoptosis in lung cancer.

IGFBP-rP1 was considered to induce neuroendocrine (NE) differentiation in interaction with a novel protein 25.1 in lung cancer and prostate cancer (33,34). Again, in prostate cancer, overexpression of the transcription factor SOX9 was thought to contribute to growth regulation by IGFBP-rP1 via inhibition of cell growth and promotion of differentiation (35). In the present study, we established a lung cancer differentiation cell-model by treating three lung cancer cell lines with the differentiation inducing agent BrdU. Exposure of SCLC cell line H526 to BrdU induced a phenotypic transition toward an epithelioid phenotype. This morphological transformation led to the development of an adherent monolayer (H526B) from spherical tightly aggregated cell –cell clusters of the non-substrate-adherent parental cell line (H526). Enhanced expression of IGFBP-rP1 was confirmed by RT-PCR and Western blot analysis in cell line H2228 and H526 after BrdU modification, indicating a role that IGFBP-rP1 plays in the process of lung cancer differentiation. However, the precise function of IGFBP-rP1 in lung cancer differentiation still remains to be investigated.

In summary, our data strengthen the observation that IGFBP-rP1 functions as a putative tumor suppressor gene via DNA methylation and induction of apoptosis in human lung cancer. The role of IGFBP-rP1 in apoptosis as well as in lung cancer differentiation could provide a potential novel therapeutic target in lung cancer.

Acknowledgements

We thank Dr. Yu for the TMA construction and Mrs. C. Scholz for photographing. We are much indebted to Martina Eickmann for secretarial assistance and critical reading. This work was supported by a grant from the Deutsche Krebshilfe (grant 10-2210-Pe 4).

References:

1. Burger AM, Leyland-Jones B, Banerjee K, Spyropoulos DD, Seth AK. Essential roles of IGFBP-3 and IGFBP-rP1 in breast cancer. Eur J Cancer 2005;41:1515-27.
2. Murphy M, Pykett MJ, Harnish P, Zang KD, George DL. Identification and characterization of genes differentially expressed in meningiomas. Cell Growth Differ 1993;4:715-22.
3. Swisshelm K, Ryan K, Tsuchiya K, Sager R. Enhanced expression of an insulin growth factor-like binding protein (mac25) in senescent human mammary epithelial cells and induced expression with retinoic acid. Proc Natl Acad Sci U S A 1995; 92:4472-6.
4. Rosenfeld RG, Oh Y. The blind men and the elephant--a parable for the study of insulin-like growth factor binding proteins. Endocrinology 1998;139:5-7.
5. Baxter RC, Binoux MA, Clemmons DR et al. Recommendations for nomenclature of the insulin-like growth factor binding protein superfamily. J Clin Endocrinol Metab 1998;83:3213.
6. Kim HS, Nagalla SR, Oh Y, Wilson E, Roberts CT Jr, Rosenfeld RG. Identification of a family of low-affinity insulin-like growth factor binding proteins (IGFBPs): characterization of connective tissue growth factor as a member of the IGFBP superfamily. Proc Natl Acad Sci U S A 1997;94:12981-6.
7. Degeorges A, Wang F, Frierson HF Jr, Seth A, Sikes RA. Distribution of IGFBP-rP1 in normal human tissues. J Histochem Cytochem 2000;48:747-54.
8. Kim JG, Kim MH, Kim IS, et al. Decreased expression of mac25 mRNA in uterine leiomyomata compared with adjacent myometrium, Am J Reprod Immunol 2000;43:53-7.

9. Mutaguchi K, Yasumoto H, Mita K, et al. Restoration of insulin-like growth factor binding protein-related protein 1 has a tumor-suppressive activity through induction of apoptosis in human prostate cancer. Cancer Res 2003;63:7717-23.
10. Sprenger CC, Damon SE, Hwa V, Rosenfeld RG, Plymate SR. Insulin-like growth factor binding protein-related protein 1 (IGFBP-rP1) is a potential tumor suppressor protein for prostate cancer. Cancer Res 1999;59:2370-5.
11. Landberg G, Ostlund H, Nielsen NH, Roos G, Emdin S, Burger AM. Downregulation of the potential suppressor gene IGFBP-rP1 in human breast cancer is associated with inactivation of the retinoblastoma protein, cyclin E overexpression and increased proliferation in estrogen receptor negative tumors. Oncogene 2001;20:3497-505.
12. Wilson HM, Birnbaum RS, Poot M, Quinn LS, Swisshelm K. Insulin-like growth factor binding protein-related protein 1 inhibits proliferation of MCF-7 breast cancer cells via a senescence-like mechanism. Cell Growth Differ 2002;13:205-13.
13. Komatsu S, Okazaki Y, Tateno M, et al. Methylation and downregulated expression of mac25/insulin-like growth factor binding protein-7 is associated with liver tumorigenesis in SV40T/t antigen transgenic mice, screened by restriction landmark genomic scanning for methylation (RLGS-M). Biochem Biophys Res Commun 2000; 267:109-17.
14. Petersen S, Heckert C, Rudolf J, et al. Gene expression profiling of advanced lung cancer. Int J Cancer 2000;86:512-7.
15. Difilippantonio S, Chen Y, Pietas A, et al. Gene expression profiles in human non-small and small-cell lung cancers. Eur J Cancer 2003;39:1936-47.
16. Jaques G, Kiefer P, Schoneberger HJ, et al. Differential expression of insulin-like growth factor binding proteins in human non-small cell lung cancer cell lines. Eur J Cancer 1992;28:1899-904.

17. Wegmann BR, Schoneberger HJ, Kiefer PE, Jaques G, Brandscheid D, Havemann K. Molecular cloning of IGFBP-5 from SCLC cell lines and expression of IGFBP-4, IGFBP-5 and IGFBP-6 in lung cancer cell lines and primary tumours. Eur J Cancer 1993;29:1578-84.
18. Chen Y, Huhn D, Knosel T, Pacyna-Gengelbach M, Deutschmann N, Petersen I. Downregulation of connexin 26 in human lung cancer is related to promoter methylation. Int J Cancer 2005;113:14-21.
19. Micheli MR, Bova R, Pascale E, D'Ambrosio E. Reproducible DNA fingerprinting with the random amplified polymorphic DNA (RAPD) method. Nucleic Acids Res 1994;22:1921-2.
20. Sobin LH, Wittekind Ch, eds. TNM classification of malignant tumors, 5th ed. New York: Wiley-Liss, 1997. p.227.
21. Petersen S, Wolf G, Bockmuhl U, Gellert K, Dietel M, Petersen I. Allelic loss on chromosome 10q in human lung cancer: association with tumour progression and metastatic phenotype. Br J Cancer 1998;77:270-6.
22. Feyles V, Sikora, LKJ, McGarry RC, Jerry LM. Effect of retinoic acid and bromodeoxyuridine on human melanoma-associated antigen expression in small lung carcinoma cells. Oncology 1991;48:58-64.
23. Thomas L, Chan PW, Chang S, Damsky C. 5-Bromo-2'-deoxyuridine regulates invasiveness and expression of integrins and matrix-degrading proteinases in a differentiated hamster melanoma cell. J Cell Sci 1993;105:191-201.
24. Walsh D, Meleady P, Power B, Morley SJ, Clynes M. Increased levels of the translation initiation factor eIF4E in differentiating epithelial lung tumor cell lines. Differentiation 2003;71:126-34.

25. Burger AM, Zhang X, Li H, et al. Down-regulation of T1A12/mac25, a novel insulin-like growth factor binding protein related gene, is associated with disease progression in breast carcinomas. Oncogene 1998;16:2459-67.
26. Chang YS, Wang L, Suh YA, et al. Mechanisms underlying lack of insulin-like growth factor-binding protein-3 expression in non-small-cell lung cancer. Oncogene 2004;23:6569-80.
27. Hwa V, Tomasini-Sprenger C, Bermejo AL, Rosenfeld RG, Plymate SR. Characterization of insulin-like growth factor-binding protein-related protein-1 in prostate cells. J Clin Endocrinol Metab 1998;83:4355-62.
28. Haugk KL, Wilson HM, Swisshelm K, Quinn LS. Insulin-like growth factor (IGF)-binding protein-related protein-1: an autocrine/paracrine factor that inhibits skeletal myoblast differentiation but permits proliferation in response to IGF. Endocrinology 2000;14:100-10.
29. Oh Y. IGF-independent pendent regulation of breast cancer growth by IGF binding proteins. Breast Cancer Res Treat 1998;47:283-93.
30. Lee HY, Chun KH, Liu B, et al. Insulin-like growth factor binding protein-3 inhibits the growth of non-small cell lung cancer. Cancer Res 2002;62:3530-7.
31. Liu C, Lian F, Smith DE, Russell RM, Wang XD Lycopene supplementation inhibits lung squamous metaplasia and induces apoptosis via up-regulating insulin-like growth factor-binding protein 3 in cigarette smoke-exposed ferrets. Cancer Res 2003; 63:3138-44.
32. Sueoka N, Lee HY, Wiehle S, et al. Insulin-like growth factor binding protein-6 activates programmed cell death in non-small cell lung cancer cells. Oncogene 2000; 19:4432-6.

33. Walker GE, Antoniono RJ, Ross HJ, Paisley TE, Oh Y. Neuroendocrine-like differentiation of non-small cell lung carcinoma cells: regulation by cAMP and the interaction of mac25/IGFBP-rP1 and 25.1. Oncogene 2006;25:1943-54.
34. Wilson EM, Oh Y, Hwa V, Rosenfeld RG. Interaction of IGF-binding protein-related protein 1 with a novel protein, neuroendocrine differentiation factor, results in neuroendocrine differentiation of prostate cancer cells. J Clin Endocrinol Metab 2001; 86:4504-11.
35. Drivdahl R, Haugk KH, Sprenger CC, Nelson PS, Tennant MK, Plymate SR. Suppression of growth and tumorigenicity in the prostate tumor cell line M12 by overexpression of the transcription factor SOX9. Oncogene 2004;23:4584-93.

Figure legends

Figure 1. A, Northern blot analysis of IGFBP-rP1 mRNA from cultured normal epithelial lung cells (HBEC), normal small airway epithelial cells (SAEC) and lung cancer cell lines. IGFBP-rP1 mRNA was underexpressed in lung cancer cell lines in contrast to HBEC and SAEC. Lower panel: Control hybridization with β-actin. B, RT-PCR demonstrated the decreased expression of IGFBP-rP1 mRNA in lung cancer cell lines compared to HBEC and SAEC. N: Negative control (H_2O as template). Lower panel: GAPDH was used as a positive control. C, Western blot analysis of IGFBP-rP1 protein expression in HBEC and lung cancer cell lines. Compared to HBEC, most of the lung cancer cell lines showed diminished expression of IGFBP-rP1.

Figure 2. Examples of IGFBP-rP1 protein expression in primary lung tumors. A section from TMA (A, 2.5 fold magnification); IGFBP-rP1 negative (B, 25 fold magnification); IGFBP-rP1 weakly positive (C, 25 fold magnification); IGFBP-rP1 moderately positive (D, 25 fold magnification); IGFBP-rP1 strongly positive (E, 25 fold magnification).

Figure 3. A, RT-PCR showed the rexpression of IGFBP-rP1 in lung cancer cell lines H2170, H226 and SHP77 after exposure to demethylation agent, 5-aza-2'-deoxycytidine. The concentration of 5-aza-2'-deoxycytidine was indicated. cDNA from HBEC was used as positive control (P). Lower panel: The integrity of RNA and cDNA was confirmed using GAPDH as positive control. B, PCR using the bisulfite modified genomic DNA isolated from HBEC, H2170, H226 and SHP77 as templates. In bisulfite treated DNA, a 186-bp target band of IGFBP-rP1 was found, while in unmodified DNA (N), there was no specific band detectable.

Figure 4. A**,** Western blot analysis of protein isolated from media. IGFBP-rP1 protein expression was found in cells of N6 and N10 stably transfected with full-length cDNA of IGFBP-rP1. In mock tranfectants (M12 and M18) as well as in parental cells H2170, no signal detectable. B, Colony formation assay. IGFBP-rP1 transfectants N6 and N10 showed reduced capacity to form colonies in soft agar compared to negative controls. C, Tumorigenicity assay in immune-deficient nude mice. IGFBP-rP1 transfectants N6 and N10 suppressed tumor grow rate in nude mice compared to controls.

Figure 5. Effect of IGFBP-rP1 expression on apoptotic index of H2170 cells**.** A, Typical photographic demonstration of apoptotic cell count in IGFBP-rP1-positive clone of N10, mock transfectant M12 and parental cells H2170. B, The number of apoptotic cells in IGFBP-rP1 transfectant N10 (42 out of 100) is higher than that in mock transfectant M12 (8 of 100) and parental cells H2170 (4 of 100 cells; $p<0.001$). C, Up-regulation of caspase-3 was observed in IGFBP-rP1 transfected cells of N10 compared to controls.

Figure 6. Role of IGFBP-rP1 in lung cancer differentiation. A, H526 cells were treated with BrdU as described under Materials and Methods to develop the stable adherent H526B cell line. Phase contrast micrograph of H526 cell aggregates in suspension. B, Phase contrast micrograph showing the epithelioid morphology of H526B cell monolayer. C, DNA fingerprinting of H526 and H526B cell lines showing the same DNA banding pattern between these two cells by using primer sets 4 and 5. D, IGFBP-rP1 was upregulated at mRNA level in the cell line H2228 and H526 after BrdU treatment. E, increased IGFBP-rP1 protein was observed in the cell line H2228 and H526 after BrdU modification.

Table 1. Study cohort.

Table 2. Methylation patterns of IGFBP-rP1 from aberrantly methylated lung tumor cell lines. Sequencing of colonies from H2170, H226 and SHP77 revealed a heterogeneous methylation status. methylated CpG dinucleotides are indicated by closed circles; Open circles represent the unmethylated CpG dinucleotides;

Table 3. Correlation between IGFBP-rP1 protein expression and clinicopathological data.

Table 1 Study cohort

	IGFBP-7 negative n (%)	IGFBP-7 positive n (%)
Total No (n = 138)	58(42%)	80(58%)
ADC	29(21%)	39(28%)
SCC	25(19%)	34(25%)
LCLC	2(1%)	5(4%)
SCLC	2(1%)	2(1%)
Grade 1-2	32(23%)	34(25%)
Grade 3	26(19%)	46(33%)
PT1	13(9%)	21(15%)
PT2+	45(33%)	59(43%)
PN0	34(25%)	41(30%)
PN1+	24(17%)	39(28%)
Stage I-II	38(28%)	54(39%)
Stage III-IV	20(14%)	26(19%)

ADC=adenocarcinomas; SCC=squamous cell carcinoma; LCLC= large cell lung carcinoma; SCLC= small cell lung carcinoma

Table 2 Methylation patterns of IGFBP-rP1 from aberrantly methylated lung tumor cell lines.

Colonies \ CpG position	502	517	521	541	544	548	556	569	572	577	581	583	586	592	597	599	611	620	622
H2170-1	○	○	●	●	●	●	●	●	●	○	●	○	●	○	○	●	○	○	○
H2170-2	●	●	○	●	●	○	●	○	●	○	○	○	○	○	○	○	○	○	●
H2170-3	○	○	○	○	●	○	●	○	○	○	○	○	○	○	○	○	○	○	○
H2170-4	○	○	○	●	●	●	●	●	●	●	●	○	●	○	○	○	○	○	○
H2170-5	○	○	○	●	●	●	●	●	○	○	●	○	●	○	○	○	○	○	○
H2170-6	○	●	●	●	●	●	●	●	●	●	●	●	○	○	○	○	○	○	○
H2170-7	○	○	○	●	●	●	●	○	●	●	●	○	●	○	○	○	○	○	○
H2170-8	●	○	○	○	●	○	●	○	●	○	●	●	●	○	○	○	○	●	●
H2170-9	○	○	●	●	●	●	●	●	●	○	●	○	●	○	○	●	○	○	○
H2170-10	○	○	●	●	●	●	●	●	●	○	●	○	●	○	○	●	○	○	○
H2170-11	○	○	●	●	●	●	●	●	●	○	●	○	●	○	○	●	○	○	○
H2170-12	○	○	●	●	●	●	●	●	●	○	●	○	●	○	○	●	○	○	○
H2170-13	○	○	●	●	●	●	●	●	●	○	●	○	●	○	○	●	○	○	○
H2170-14	○	○	●	●	●	●	●	●	●	○	○	○	●	○	○	●	○	○	○
H2170-15	○	○	●	●	●	●	●	●	●	○	○	○	●	○	○	●	○	○	○
H2170-16	○	○	●	●	●	●	●	●	●	○	●	○	●	○	○	●	○	○	○
H2170-17	○	○	●	●	●	●	●	●	●	○	●	○	●	○	○	●	○	○	○
H2170-18	○	○	●	●	●	●	●	●	●	○	●	○	●	○	○	●	○	○	○
H2170-19	○	○	●	●	●	●	●	●	●	○	●	○	●	○	○	●	○	○	○
H2170-20	○	○	●	●	●	●	●	●	●	○	●	○	○	○	○	●	○	○	○
H226-1	●	●	●	●	●	●	●	●	●	●	●	●	●	●	●	●	●	●	●
H226-2	○	○	○	●	●	●	●	●	●	○	●	○	●	○	○	●	○	○	○
H226-3	○	○	●	●	●	●	●	●	●	○	●	○	●	○	○	●	○	○	○
H226-4	○	○	●	●	●	●	●	●	●	○	●	○	●	○	○	●	○	○	○
H226-5	○	○	●	●	●	●	●	●	●	○	●	○	●	○	○	●	○	○	○
H226-6	○	○	●	●	●	●	●	●	●	○	●	○	●	○	○	●	○	○	○
H226-7	○	○	●	●	●	●	●	●	●	○	●	○	●	○	○	●	○	○	○
H226-8	○	○	●	●	●	●	●	●	●	●	●	●	●	●	●	●	●	●	●
H226-9	○	○	●	●	●	●	●	●	●	○	●	○	●	○	○	●	○	○	○
H226-10	○	○	●	●	●	●	●	●	●	○	●	○	●	○	○	●	○	○	○
H226-11	○	○	●	●	●	●	●	●	●	○	●	○	●	○	○	●	○	○	○
H226-12	○	○	●	●	●	●	●	●	●	○	●	○	●	○	○	●	○	○	○
H226-13	○	○	●	●	●	●	●	●	●	○	●	○	●	○	○	●	○	○	○
H226-14	○	○	●	●	●	●	●	●	●	○	●	○	●	○	○	●	○	○	○
H226-15	○	○	●	●	●	●	●	●	●	○	●	○	●	○	○	●	○	○	○
H226-16	○	○	●	●	●	●	●	●	●	○	●	○	●	○	○	●	○	○	○
H226-17	○	○	●	●	●	●	●	●	●	○	●	○	●	●	●	●	○	○	○
H226-18	○	○	●	●	●	●	●	●	●	○	●	○	●	○	○	●	○	○	○
H226-19	○	○	●	●	●	●	●	●	●	○	●	○	●	○	○	●	○	○	○
H226-20	○	○	●	●	●	●	●	●	●	●	●	○	●	○	○	●	○	○	○
SHP77-1	●	●	●	●	●	●	●	●	●	●	●	●	●	●	●	○	●	●	●
SHP77-2	○	○	○	●	●	●	●	●	●	●	●	●	●	●	●	●	●	●	●
SHP77-3	●	○	●	●	●	●	●	●	●	○	●	●	●	○	●	●	●	●	●
SHP77-4	●	●	●	○	●	●	●	●	●	●	●	●	●	●	●	●	●	●	●
SHP77-5	●	●	●	●	●	●	●	●	●	●	●	●	●	●	●	●	●	●	●
SHP77-6	●	●	●	●	●	●	●	●	●	○	●	●	●	○	●	●	●	●	●
SHP77-7	●	○	●	○	●	●	●	○	●	●	●	●	●	●	●	●	●	●	●
SHP77-8	●	●	●	●	●	●	●	○	●	●	●	●	●	●	●	●	●	●	●
SHP77-9	○	○	●	●	●	●	●	●	●	●	●	●	●	●	●	●	●	●	●
SHP77-10	●	●	●	●	●	●	●	●	●	●	●	●	●	●	●	●	●	●	●
SHP77-11	○	○	●	●	●	●	●	●	●	○	○	○	●	○	○	●	○	○	○
SHP77-12	○	○	●	●	●	●	●	●	●	○	●	○	●	○	○	●	○	○	○
SHP77-13	○	○	●	●	●	●	●	●	●	○	●	○	●	○	○	●	○	○	○
SHP77-14	○	○	●	●	●	●	●	●	●	○	●	○	●	○	○	●	○	○	○
SHP77-15	○	○	●	●	●	●	●	●	●	●	●	●	●	●	●	●	●	●	●
SHP77-16	○	○	●	●	●	●	●	●	●	○	○	○	○	○	○	○	○	○	○
SHP77-17	○	○	●	●	●	●	●	●	●	○	●	○	●	○	○	●	○	○	○
SHP77-18	○	○	●	●	●	●	●	●	●	○	●	○	●	○	○	●	○	○	○
SHP77-19	○	○	●	●	●	●	●	●	●	○	○	○	●	○	○	●	○	○	○
SHP77-20	○	○	●	●	●	●	●	●	●	○	●	○	●	○	○	●	○	○	○

Table 3 Correlation between IGFBP-rP1 expression and clinicopathological data (p values*)

	Stage (UICC)	**Grade**	**pN+**	**pT**
ADC	0.445	1,000	0.807	0.070
SCC	0.275	0.029	0.169	0.061
All tumours	0.856	0.168	0.489	0.691

*P values were calculated by Chi-square test

ADC = adenocarcinoma; SCC = squamous cell carcinoma

Fig. 1A

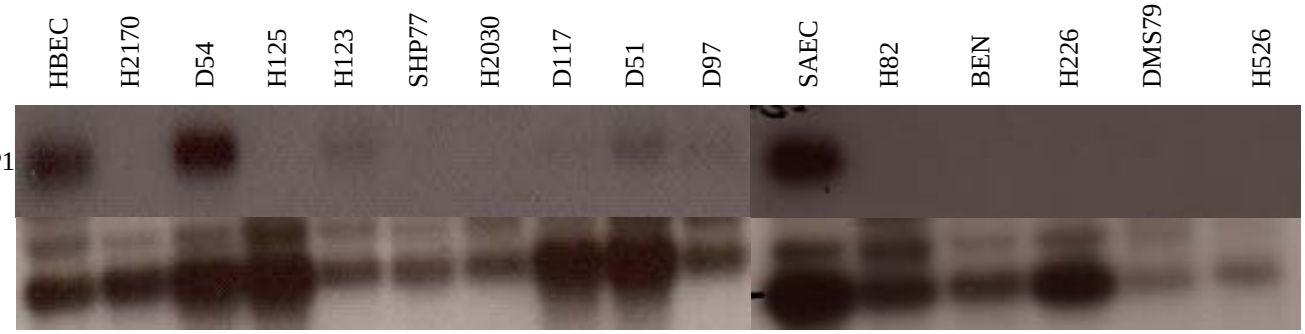

Fig. 1B

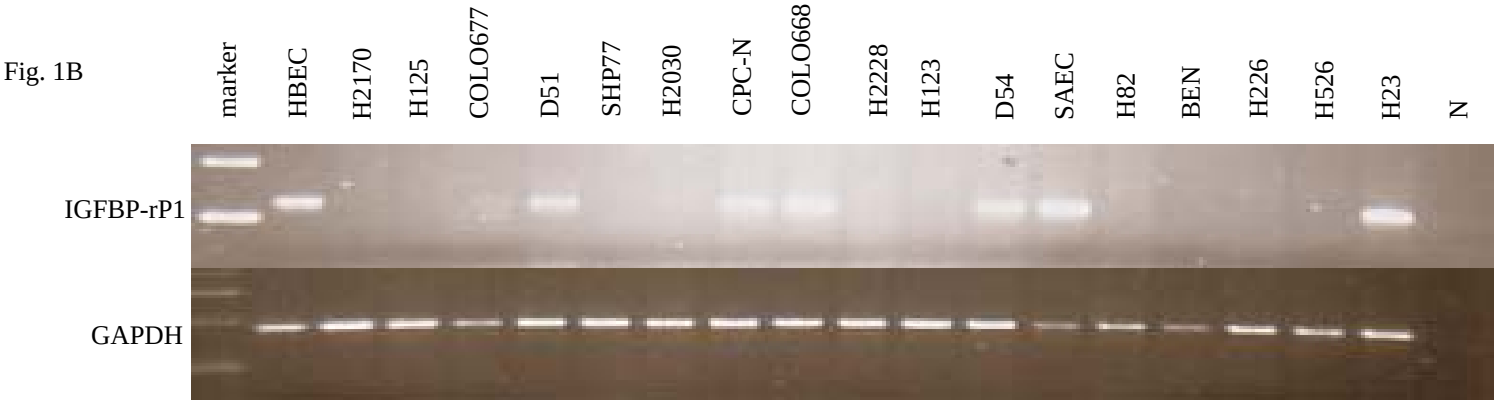

Fig. 1C

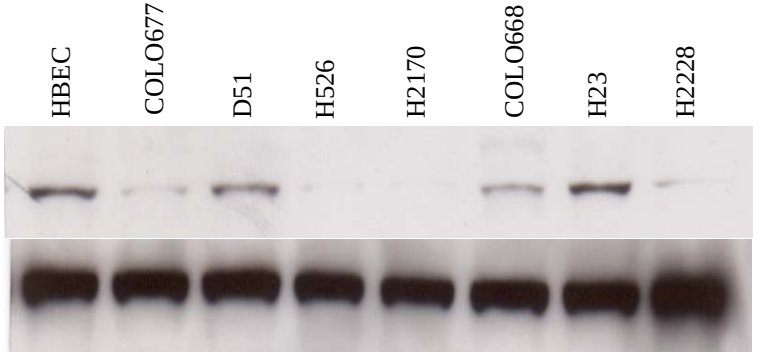

Fig.2

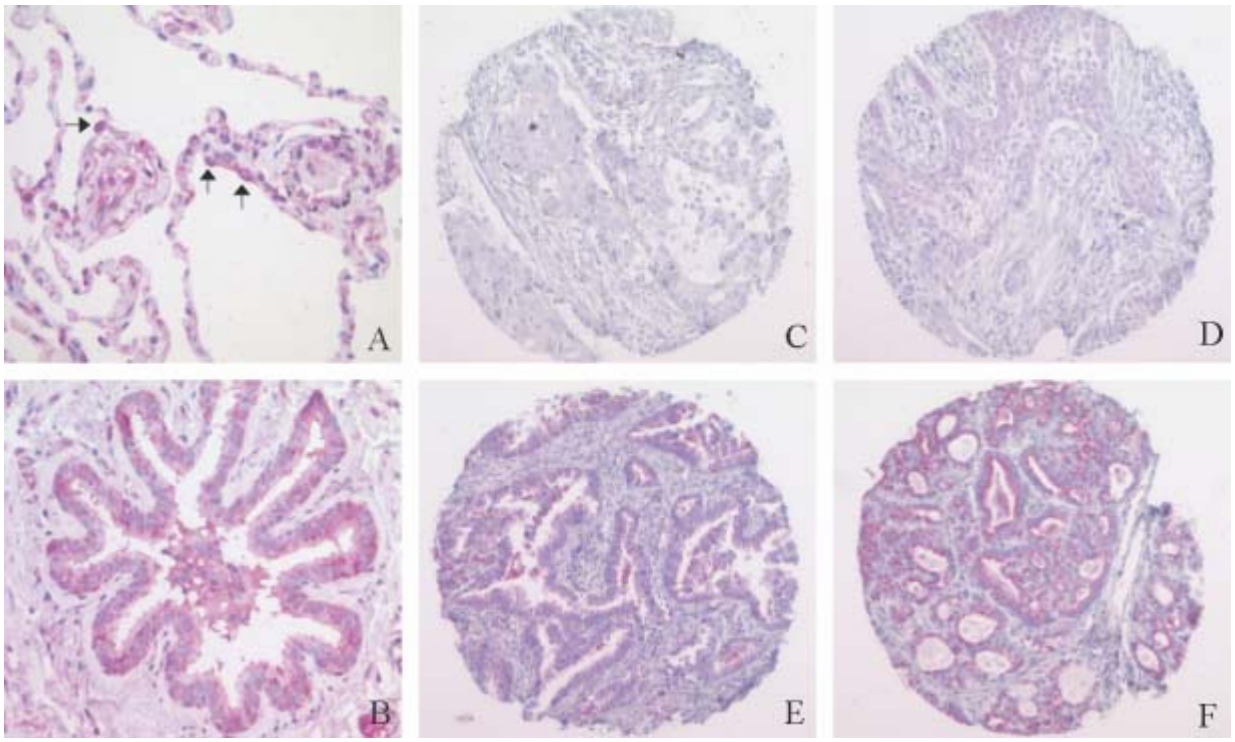

Fig. 3A

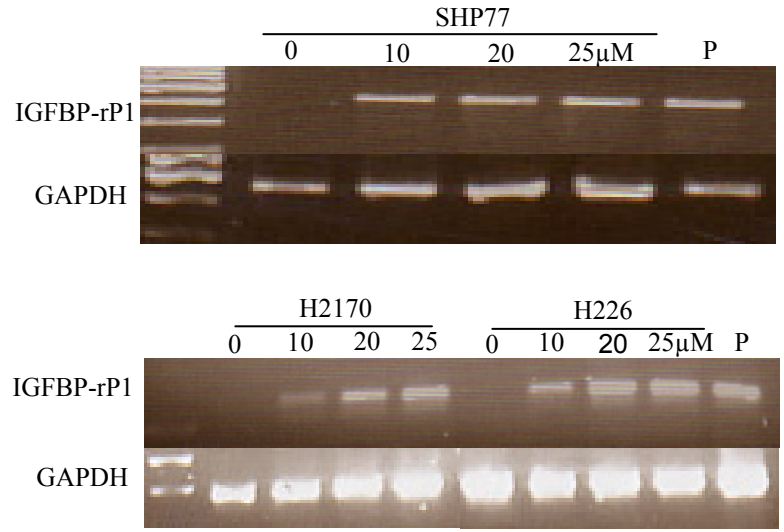
SHP77
0
10
20
25μM
P
IGFBP-rP1
GAPDH
H2170
H226
0
10
20
25
0
10
20
25μM
P
IGFBP-rP1
GAPDH

Fig. 3B

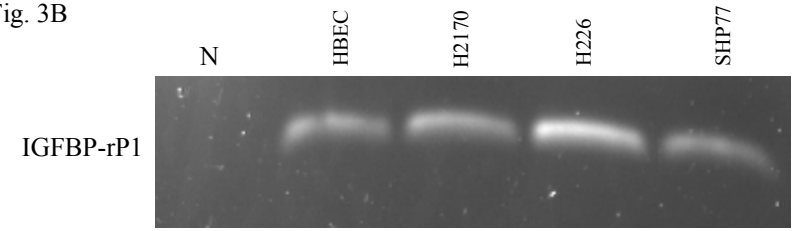
N
HBEC
H2170
H226
SHP77
IGFBP-rP1

Fig. 4A

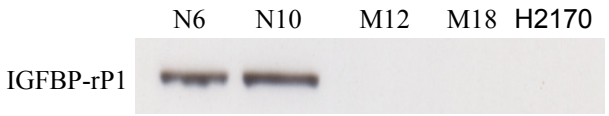

Fig. 4B

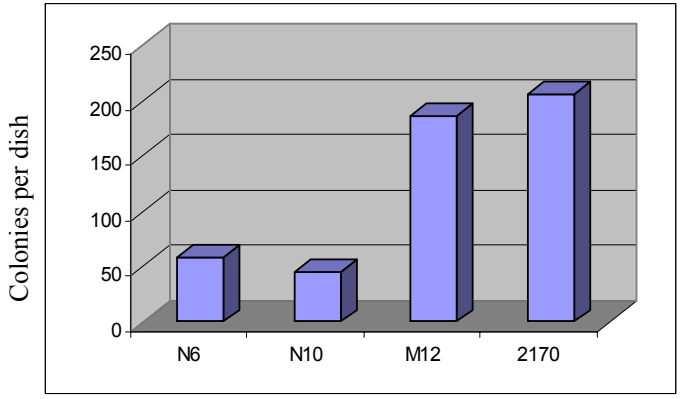

colony-formation assay in soft agar

Fig. 4C

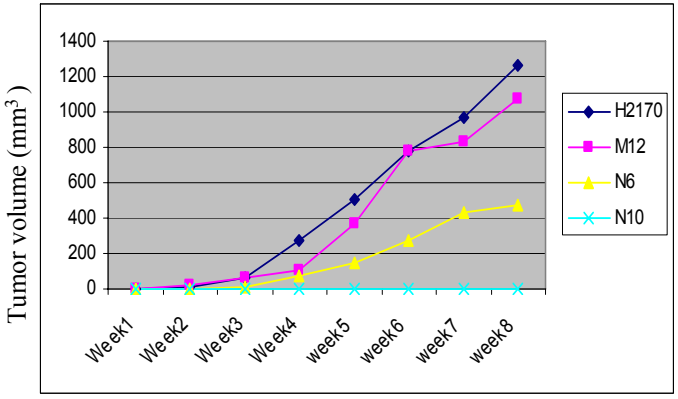

tumorigenicity in immune-deficient nude mice

Fig. 5A

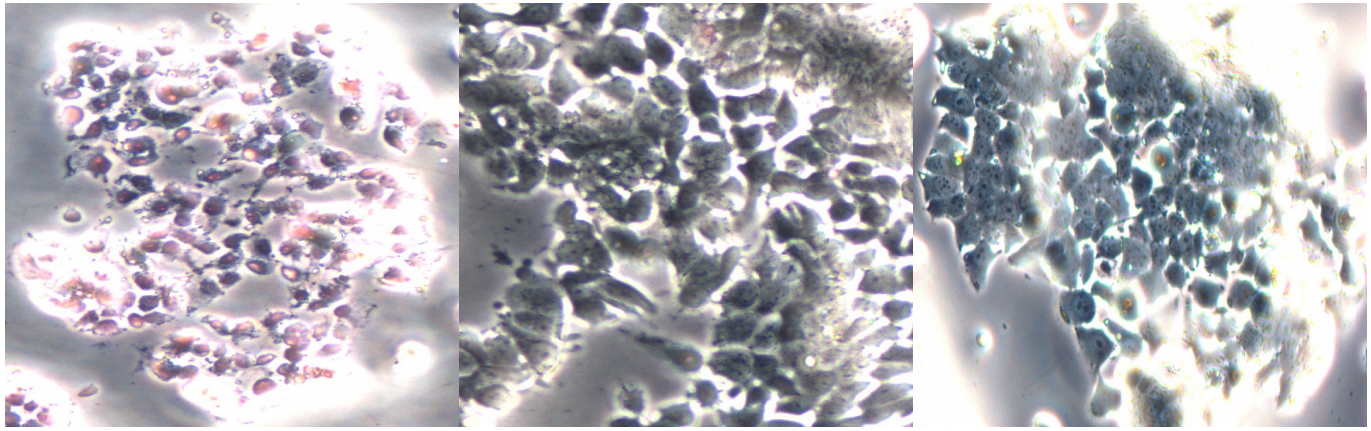

Fig. 5B

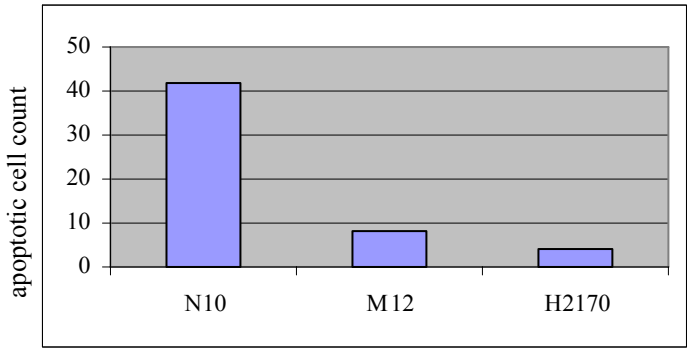

Fig. 5C